

Supporting Information for

Selective preconcentration and online collection of charged molecules
using ion concentration polarization

Jihye Choi, Keon Huh, Dustin Jaesuk Moon, Hyomin Lee, Seok Young Son, Kihong Kim,
Hee Chan Kim, Jong-Hee Chae, Gun Yong Sung, Ho-Young Kim,
Jong Wook Hong and Sung Jae Kim

1. Microchamber design

In this work, repeated microchamber structures have been employed, since (1) they can suppress unwanted expansion of the ion depletion zone and vortices, (2) the electric field varies strong/weak repeatedly for easy trapping and (3) they can cut the tail of preconcentrated plugs for clear visualization. Both experimental and numerical analysis for supporting this structure are as following.

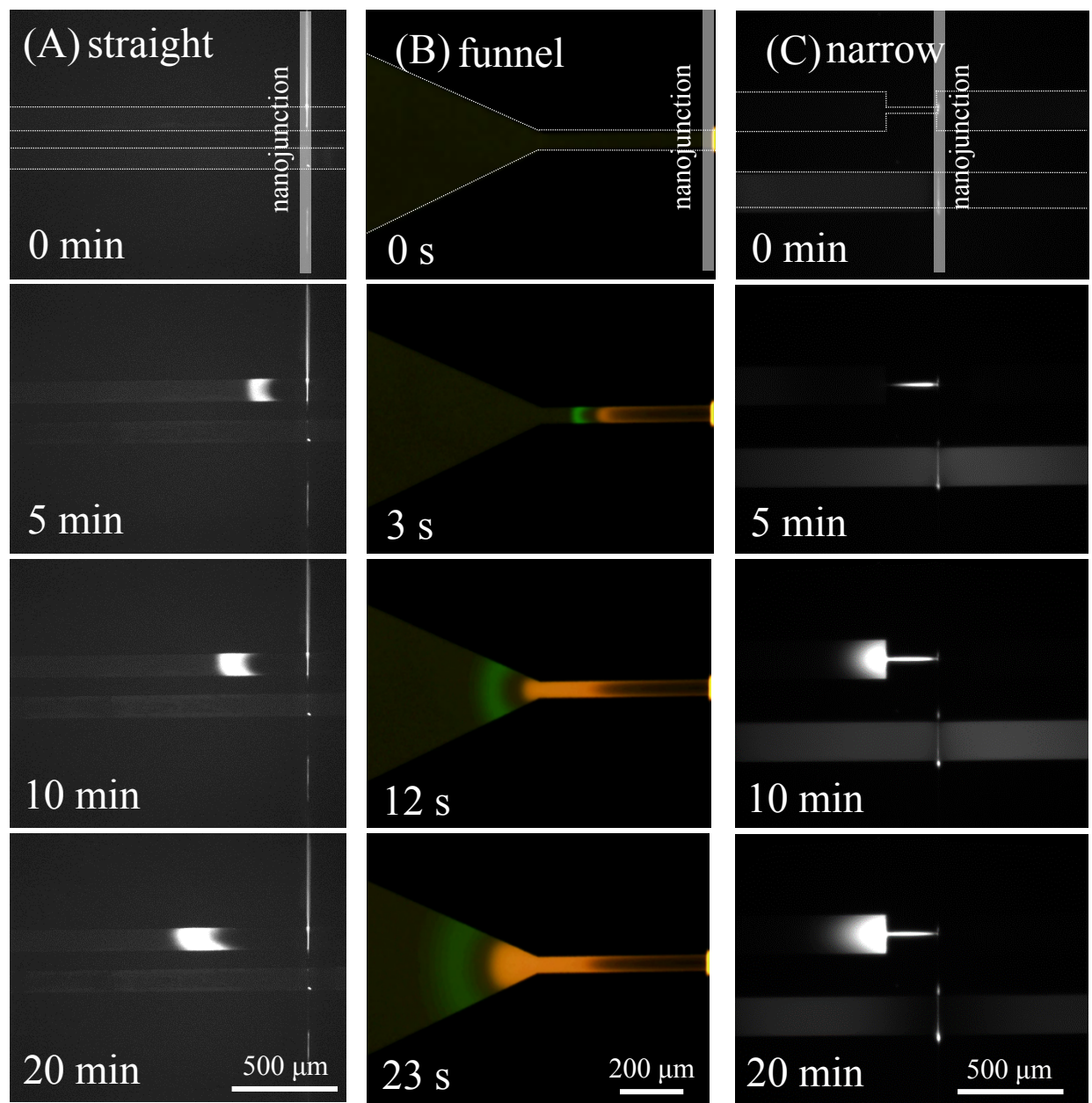
1.1 Experimental analysis of preconcentration behavior for various microchannel geometries

As shown in SI Figure 1(A), molecules were highly preconcentrated near the boundary of the ion depletion zone in a straight channel, while the preconcentrated plug kept propagating toward the reservoir along the boundary of the depletion zone. Because of the following extraction system, pinning the location of plugs was critical issue in our system and we had tried to resolve this by manipulating the strength of electrical field using various microchannel geometries such as funnel and narrow shape. In a funnel channel, a preconcentrated plug was arrested at the boundary of the depletion zone which stopped expanding at the site where the channel starts to diverge. However, the second preconcentrated plug dispersed significantly as

shown in SI Figure 1(B).

In order to obtain steeper gradient an electric field¹, a narrow structure was designed as shown in SI Figure 1(C), it was found that a narrow channel close to the nanojunction curbed the ever-expanding depletion zone, *i.e.* stabilizing (or pinning) the depletion zone. Therefore the preconcentrated plug, which moved along the expanding depletion zone otherwise, pinned at each balanced site since the depletion zone was confined. Also, repeating narrow and wide channels impeded the dispersion and diffusion of the preconcentrated plug. To be specific, the difference of electric field in a narrow and a wide channel engendered the difference of velocity in each channel, which facilitated the efficiency of separation.

Therefore the repeated chamber structure is supposed to have superior performance in terms of stability, cutting off tails out of Gaussian distributed plugs and helping extraction strategy. Following theoretical analysis showed that the electrical field formed at narrow section was significantly amplified so that it can act as an energy barrier to distinguish dyes. In addition, the chamber structure can effectively prohibit the expanding depletion zone by restricting vortices in the chamber.



SI Figure 1. Preconcentration operation in (A) straight microchannel, (B) funnel microchannel and (C) narrow microchannel.

1.2 Numerical analysis of ICP layer for straight and repeated chamber structure.

For investigating the effect of repeated chamber structures, numerical simulations were conducted by COMSOL Multiphysics 4.4 as a commercial FEM (finite element method) tool. Because the ICP layer is highly nonlinear region, it is difficult to ensure the convergence and the stability of numerical solutions. To resolve the critical problem, the local electroneutrality (cation concentration is equal to anion concentration in whole domain) was adopted². Namely, thin double layer approximation and ideally cation-selective membrane were chosen to reduce the computational cost. Under the local electroneutrality constraint, independent variables such as ion concentration (c), electric potential (ψ), pressure (p), and flow fields (\mathbf{u}) were governed by the diffusion-convection equation, the current conservation, the continuity equation, and the Stokes equations³. ICP phenomena in a straight channel (4 mm in length and 150 μm in height) and a repeated chamber structure (using same geometry of experiments) were analyzed by the governing equations. For the numerical stability, the voltage configurations at inlet and outlet were set to be 5 V and 3.3 V which were enough to generate the ICP phenomena inside the microchannels. The concentrations at inlet and outlet were fixed to the bulk concentration. The flow conditions at the boundaries were set to be a zero-flow rate due to pressure balance between two reservoirs⁴. We assumed that the microchannel walls have uniform zeta potential of -100 mV of which value is usual condition on PDMS surface⁵.

The simulation results were depicted in SI Figure 2. First of all, the repeated chamber structures are able to effectively confine the ion depletion zone (dark blue region) in comparison to the straight channel as shown in SI Figure 2(A). This means that the ICP layer in the repeated chamber would be stabilized because the flow instability generated by concentration fluctuation⁶ occurs only inside the first chamber where nanojunction was installed. This is helpful to obtain the stable preconcentrated plug after the first chamber. As depicted in SI Figure 2(B), the strength of electric field was changed monotonically in the

longitudinal direction of the straight channel while the strength was altered pseudo-periodically for the repeated chambers. Electric potentials obtained from the electrical field strength were schematically illustrated in SI Figure 2(D). While monotonically increased electric potentials were observed in straight microchannel (red line), there was a (almost) plateau inside microchamber with steep changes in narrow regions (blue line). A charged species would be immobilized in this plateau region. Due to the pseudo-periodic electric field and the plateau of electric potential, the preconcentrated plug would be easily trapped in each chamber. Lastly, fast vortices were confined in the first chamber so that stable flow fields were generated beyond the chamber (SI Figure 1(C)). Thus, the alterations of ICP layer by the repeated chambers would provide effective mechanisms for a stable selective preconcentration.

SI Figure 2. Numerically simulated ICP layer for (A) concentration distribution, (B) electrical field and (C) flow field. (D) Schematic illustration for electric potential near the microchamber.

References

1. S.-H. Lee, H. Lee, T. Jin, S. Park, B. J. Yoon, G. Y. Sung, K.-B. Kim and S. J. Kim, *Nanoscale*, 2015, **7**, 936-946.
2. I. Rubinstein and B. Zaltzman, *Phys. Rev. E*, 2000, **62**, 2238-2251.
3. E. V. Dydek, B. Zaltzman, I. Rubinstein, D. S. Deng, A. Mani and M. Z. Bazant, *Physical Review Letters*, 2011, **107**, 118301.
4. J. H. Masliyah and S. Bhattacharjee, *Electrokinetic and Colloid Transport Phenomena*, Wiley, 2006.
5. B. J. Kirby and E. F. Hasselbrink, *ELECTROPHORESIS*, 2004, **25**, 203-213.
6. C. L. Druzgalski, M. B. Andersen and A. Mani, *Physics of Fluids (1994-present)*, 2013, **25**, 110804.